

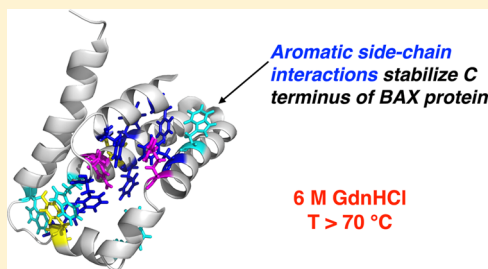
Side-Chain Packing Interactions Stabilize an Intermediate of BAX Protein against Chemical and Thermal Denaturation

Chun-Hui Chan, Chia-Jung Tsai, and Yun-Wei Chiang*

Department of Chemistry and Frontier Research Center on Fundamental and Applied Sciences of Matters, National Tsing Hua University, Hsinchu 30013, Taiwan

 Supporting Information

ABSTRACT: Bcl-2-associated X (BAX) protein plays a gatekeeper role in transmitting apoptotic signaling from cytosol to mitochondria. However, little is known about its stability. This study reports a comprehensive investigation on the stability of BAX using spin-label ESR, CD, and ThermoFluor methods. Point mutations covering all of the nine helices of BAX were prepared. ESR study shows that BAX can be divided into two structural regions, each responding differently to the presence of guanidine hydrochloride (GdnHCl). The N-terminal region (helices 1–3) is denatured in 6 M GdnHCl, whereas the C-terminal region (helices 4–9) is resistant to the denaturing effects. The far-UV CD spectra show an appreciable amount of helical content of BAX at high temperatures. The magnitude of the near-UV CD signal is increased with increasing temperature in either 0 or 6 M GdnHCl, indicating an enhancement of aromatic side-chain packing in the C-terminal region. Taken together with ThermoFluor results, we show that a core interior, wherein aromatic interactions are highly involved, within the C-terminal region plays an important role in stabilizing BAX against the denaturing effects. Collectively, we report a highly stable, indestructible intermediate state of BAX. Side-chain packing interactions are shown to be the major stabilizing force in determining BAX structure.



INTRODUCTION

Chemical denaturation, with denaturing agents such as urea and guanidine hydrochloride (GdnHCl), is one of the primary ways to investigate protein stability and unfolding.^{1–4} Despite the widespread use of the study approach, it remains unclear about the molecular basis and mechanism whereby denaturants unfold a protein. Two distinct models have been previously proposed for the mechanism of protein denaturation in aqueous solutions containing denaturants.^{2,5} In the “direct interaction” model, denaturants exert their effect directly on the protein surface by interacting with the charged hydrophilic residues and protein backbone, thereby giving rise to a swelling of the protein, exposing the hydrophobic residues, and consequently leading to a destabilization of the native state. In the “indirect model”, it has been suggested that protein denaturation occurs because denaturants preferentially solvate hydrophobic residues and lead to an effective reduction of the hydrophobic surface, which in turn destabilize the native structure of a protein. Molecular dynamics simulations of proteins in aqueous solutions containing denaturants have been interpreted in terms of both mechanisms that rely on the changes in the hydrophobic energies.^{3,6} Much of our understanding of the interactions of denaturants with protein has come from studies based on polypeptide chains, such as experiments that measure the solubility of peptide units and amino acid side chains in water, apolar solvents, and aqueous urea or GdnHCl solutions.^{7,8} In reality, the structure of a protein is determined by a delicate balance of weak interactions which, in addition to the

hydrophobic effects (e.g., aromatic interactions), include hydrogen bonds, and salt bridges. Aromatic interactions have in recent years been increasingly recognized as an important effect in stabilizing protein structure.^{9–11} Although there have been several attempts to experimentally quantitate aromatic interactions in peptides, there are far fewer such experimental studies in globular proteins.¹⁰ It remains unclear how much the side-chain interactions between aromatic residues are important in determining protein stability.

Here, we report a study of protein stability using several spectroscopic tools including continuous-wave (cw) electron spin resonance (ESR), circular dichroism (CD), and ThermoFluor techniques.^{12–15} This study explores the stability of the Bcl-2 associated X (BAX) protein.¹⁶ BAX is a member of the apoptotic group in the Bcl-2 protein family, which plays a central role in the intrinsic pathways of apoptosis. BAX is a 192 amino acid protein that contains nine helices and exists as a monomer in cytosol. Upon receipt of apoptotic signaling, cytosolic BAX proteins transform into membrane-associated oligomers, causing mitochondrial outer membrane permeabilization and then cell death. However, it remains unclear as to the stability of BAX and what structural changes (e.g., partial unfolding and refolding during the oligomerization and permeabilization) BAX is triggered to become membrane-associated complex. The stability of BAX

Received: September 9, 2014

Revised: November 18, 2014

Published: December 15, 2014



was previously investigated by CD spectroscopy.¹⁷ The thermal unfolding curves were obtained by recording the temperature dependence of the ellipticity at 222 nm, showing a modest unfolding transition with partial loss (approximately 40–50%) of its original helicity occurring within a temperature range of 70–80 °C. Interestingly, it was found that, although BAX is mainly a cytoplasmic protein, it does not denature like soluble globular proteins, many of which unfold below 70 °C. The high denaturation temperature of BAX indicates that it is a protein with a very stable structural organization, whereas chemical insights into this exceptional stability have never been reported. Likewise, understanding the stability of BAX may lead to ways of designing a molecular strategy to treat apoptosis-related diseases, since unfolding/folding of BAX is an important process during the translocation and oligomerization of BAX onto mitochondria.

MATERIALS AND METHODS

Sample Preparation. Unless specified otherwise, all chemicals used in this study were from Sigma-Aldrich, Inc. A methanethiosulfonate spin label (MTSSL; 1-oxy-2,2,5,5-tetramethyl-3-pyrroline-3-methyl) (Alexis Biochemicals, San Diego, CA) was used for the spin-labeling study. Full-length BAX and variants were prepared as we previously described.¹⁸ The typical yield (>95% purity) of the 0.15 mg/L culture could reproducibly be obtained for wild-type (wt) BAX. For cysteine mutants of BAX, the typical yield (>95% purity) was 0.15–0.05 mg/L. Wt-BAX carries two endogenous cysteine residues at sites 62 and 126. Cysteine-free BAX, which corresponds to C62A/C126A, is denoted by cf-BAX and used to prepare cysteine variants. For the spin-labeling study, recombinant BAX variants were prepared using a QuikChange mutagenesis kit (Stratagene) to bear only one cysteine residue at the indicated sites. In addition to wt-BAX and cf-BAX, there were in total 27 BAX mutants used in the cw-ESR study and 28 BAX mutants used in the ThermoFluor assay. Proteins were labeled with a 10-fold excess of the MTSSL label per cysteine residue for overnight (>12 h) in the dark at 4 °C. To remove free radicals, the spin-labeled BAX solution was dialyzed against four changes of buffer (20 mM sodium phosphate, pH 8.0, 100 mM NaCl) over 1–3 h and a final change of buffer over 24 h. The volume of the buffer is about 1000 times of the protein solution. MALDI-TOF experiments were conducted to confirm the identity of the proteins carrying the spin labels. In this study, the protein buffer was further exchanged to MOPS (20 mM MOPS, 100 mM NaCl, 20% (v/v) glycerol, pH 8), because it was reported that GdnHCl would result in abnormal dissociation of sodium phosphate, leading to an unexpected pH value.¹⁹

ThermoFluor Assay. ThermoFluor assay was conducted with the Steponeplus Real time PCR System (Life technologies Inc.).¹³ The temperature was increased from 4 to 95 °C in increments of 1 °C. The fluorescence dye Sypro Orange (Invitrogen) with emission wavelength at 625 nm (with ROX emission filter) was used. Solutions of 1 μL of 200× Sypro Orange and 14 μL of 0.21 mg/mL protein were added to each well of an eight-well thin-wall PCR plate for measurements. The equilibrium time was 5 s for each temperature. Fluorescence intensities were plotted as a function of temperature. The melting temperature (*T*_m) was determined using the negative of the first derivative (slope) of the fluorescent curve because ThermoFluor assay is designed to detect loss of fluorescence in the melting of

protein.¹³ The estimation of errors was based on three independent measurements. This study has also carried out a control experiment on several BAX variants (including wt-BAX) with and without the conjugated spin label (designated as R1 side chain). The R1 mutants (e.g., 113R1) have a similar *T*_m (within <1 °C) to the cysteine variants (e.g., 113C) of BAX, indicating that the introduced R1 side chain causes an insignificant change in the stability of the cysteine variants.

Circular Dichroism (CD) Spectroscopy. CD measurements were performed with an Aviv Model 410 circular dichroism spectrometer, using quartz cuvettes with a path length of 1 cm. The protein concentration was 0.5 μM. The equilibrium time was 5 min at each temperature. All spectra shown were corrected by subtracting the corresponding blanks. No precipitation was observed during the heating experiments.

Cw-ESR Experiments and Data Analysis. Approximately 40 μL solution volume, containing 20% (v/v) glycerol as a cryoprotectant, was added into the quartz ESR tube. The concentration of BAX in the ESR measurements was ca. 0.3–0.5 mM. The cw-ESR experiment was performed at an operating frequency of 9.4 GHz and 1.5 mW incident microwave power using a Bruker ELEXSYS E580-400 cw/pulsed spectrometer. For the thermal denaturation (30–80 °C) study by ESR, each spectrum was recorded with a magnetic width of 120 G, 1024 points, and 10 scans. Experimental spectra were analyzed by a nonlinear least-squares (NLLS) fitting program based upon the stochastic Liouville equation.^{20,21} All of the images of the BAX structures presented were created with PyMOL (version 1.7).

It has been well established that the hyperfine splitting of a nitroxide-based probe, i.e., the distance between outer extrema in the X-band cw-ESR spectrum, is very sensitive to the local environment, to the polarity and mobility of the side chain in particular.^{18,22} In the very fast motional regime,²³ in which the ESR spectrum is isotropic, the hyperfine approaches *A*₀, i.e., the average of the hyperfine tensor, and reflects largely local polarity. In the slow motional regime,²³ the anisotropy of the hyperfine is resolved in the spectrum, making the hyperfine splitting more sensitive to the mobility of the spin probe. The hyperfine is increased with a decrease in mobility of the side chain. In the present study, GdnHCl-induced change in local polarity is not important (see the Results) in affecting hyperfine splitting. Most of the obtained spectra were in the slow motional regime. Therefore, this study primarily measures the hyperfine difference between the spectra of 0 and 6 M GdnHCl to assess the local mobility of the side chain, providing a quantitative description for the local environment along the spin-labeling sites and GdnHCl concentration.

RESULTS

Cw-ESR Reveals a Stable Intermediate of BAX in 6 M GdnHCl. Wild-type BAX (wt-BAX) protein contains nine helices and carries two endogenous cysteine residues at sites 62 and 126 (Figure 1A). No disulfide bond has been reported between the two cysteine residues. Wt-BAX was mutated to prepare a cysteine-free BAX (cf-BAX), i.e., C62A/C126A, for the following spin-labeling study. A nitroxide-based MTSSL side chain (designated as R1) was attached covalently to a cysteine introduced on a cf-BAX through site-specific mutagenesis (see the Materials and Methods). In total, we

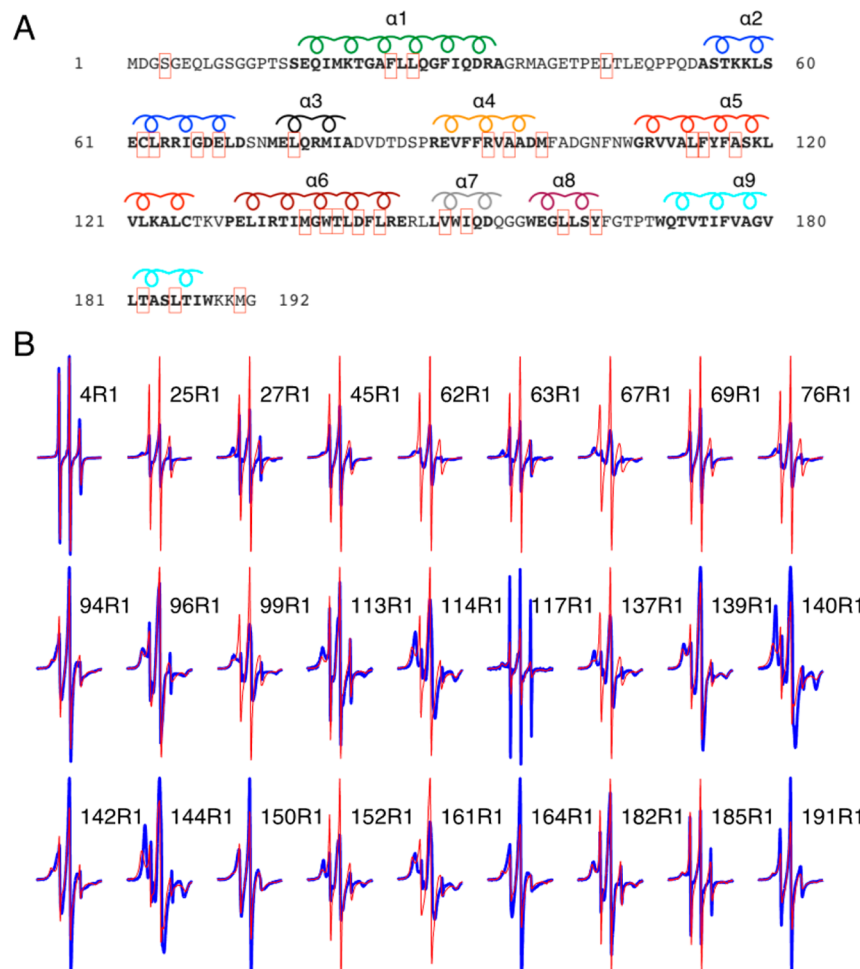


Figure 1. (A) The sequence of mouse wt-BAX protein. The sites, which were mutated to cysteine to form disulfide bonds with the MTSSL probe (designated as R1), are highlighted with red boxes. The sites cover all of the helices of BAX. (B) Normalized cw-ESR spectra of the spin-labeled cysteine mutants, covering all of the nine helices, were obtained at 25 °C in 0 M (blue) and 6 M (red) GdnHCl. The spectra were normalized to have the same double integration. The width of the displayed spectra is 100 G.

have 27 single-cysteine variants of BAX, each of which carries one R1 side chain at the indicated sites (denoted by red boxes in Figure 1A) on BAX protein. Cw-ESR spectra of the singly labeled BAX mutants were obtained in 0 and 6 M GdnHCl at temperatures of 25 °C (Figure 1B), 2 °C, and -23 °C. (See Figures S1–S4, Supporting Information, wherein the studied sites corresponding to a buried or solvent-exposed environment within BAX are clearly denoted.) All spectra in Figure 1B are normalized to have the same double integration, giving a better indication for the change of local mobility. A comparison of the normalized spectra between 0 and 6 M GdnHCl conditions shows that spectra corresponding to the first nine mutation sites from the N-terminus (i.e., 4, 25, 27, 45, 62, 63, 67, 69, and 76 which are within $\alpha 1-\alpha 3$ and are, hereafter, called the N-terminal region (NTR)) display a typical line shape of a highly mobile environment (characterized by three sharp peaks and of greater spectral magnitude) in 6 M GdnHCl (red in Figure 1B), in accord with our expectation that protein becomes denatured in the presence of high GdnHCl and the mobility of the local environment is increased accordingly. (The differences between the spectra obtained in 0 and 6 M GdnHCl for the NTR are even more substantial at lower temperatures, shown in Figures S1 and S2, Supporting Information.) Spectra

of 4R1 display an isotropic line shape and change little between 0 and 6 M GdnHCl, indicating that the N-terminus is highly mobile and the presence of 6 M GdnHCl causes an insignificant change in local polarity (cf. Materials and Methods); spectral changes observed in this BAX study reflect largely the local mobility of the side chains. Strikingly, spectra corresponding to residues within and after $\alpha 4$ (i.e., the region of residue numbers after 89 and is, hereafter, called the C-terminal region (CTR)) were generally observed to exhibit an increased immobilization after the addition of 6 M GdnHCl. ESR spectra clearly show that the N- and C-terminal regions respond differently to the presence of GdnHCl.

To provide a quantitative description for the spectral changes and relate the changes to local environment, hyperfine splitting (as illustrated in Figure S5, Supporting Information) and its change in response to the presence of GdnHCl were obtained (Figure 2A).^{24,25} (See also Figure S6, Supporting Information, for the determination of hyperfine in the experimental spectra corresponding to 6 M GdnHCl.) The plot of the hyperfine changes (Figure 2A) exhibits that, as GdnHCl is present, hyperfine of the spectra from the NTR is decreased substantially (except for the sites, 45 and 69, which were intrinsically highly solvent-exposed within native

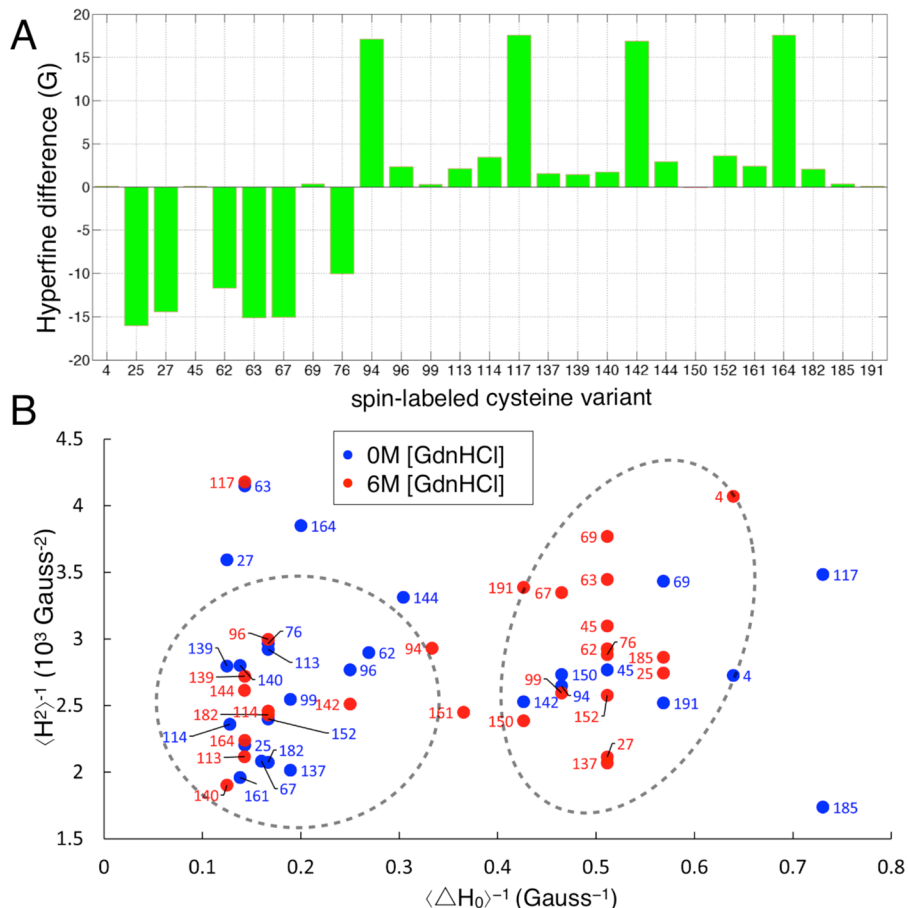


Figure 2. (A) Hyperfine difference plot. Positive and negative values of the difference indicate the increased and decreased hyperfine, respectively, in response to the presence of 6 M GdnHCl. A decreased value in hyperfine indicates an increase in the mobility of the local environment of the R1 side chain, in agreement with a general expectation for protein unfolding. An increased value of hyperfine suggests that the local structure is not denatured in response to the presence of GdnHCl. (B) Hubbell plot of the BAX variants in 0 and 6 M GdnHCl. Dashed circles correspond to a highly immobilized state (left-hand side) and a mobile state (right-hand side) of the R1 side chain. The majority of the sites in the CTR became clustered in the left-hand-side circle upon the presence of GdnHCl, suggesting the side-chain packing in the CTR is increased.

BAX), consistent with our expectation that the NTR is denatured in 6 M GdnHCl. However, hyperfine of the spectra from the CTR is generally increased, indicating an increased immobilization and local ordering. It is counterintuitive that the presence of GdnHCl generally enhances the immobilization of the R1 side chains in the CTR.

In 6 M GdnHCl, spectra in the NTR consistently exhibit a typical fast motional line shape, which is characterized by three sharp and distinct peaks, and the corresponding hyperfine values appear close to each other within 34.95 ± 0.25 G, suggesting that the local environment becomes highly similar and mobile after the GdnHCl-induced denaturation.²⁵ For the sites in the CTR, although the presence of GdnHCl brings about some changes in line width, the local environments do not appear to become highly solvent exposed and mobile. Despite a small population (ca. <8%) of the *fast* component (cf. Figure S5, Supporting Information, for details) that could be generally observed in the spectra, hyperfine was observed to increase in the spectra corresponding to the CTR. This hyperfine increase is strong evidence for the enhanced immobilized state in the presence of GdnHCl. In particular, an immobile component was observed to become visible in the spectra of 94R1, 117R1, 142R1, and 164R1 in the presence of 6 M GdnHCl (Figure S6, Supporting Information), thereby resulting in a large increase

in the hyperfine values (Figure 2A), suggesting that the presence of GdnHCl induces a relatively immobilized state of the R1 side chain in the local environment of those sites. Additionally, we note that the possibility that the immobilized state in 6 M GdnHCl was due to aggregation of the partially denatured BAX was ruled out in the experiment shown in Figure S7 (Supporting Information). It, therefore, suggests that in high GdnHCl the CTR still retains to some extent its local structures and remains packed.

The motion of the nitroxide is encoded in the ESR spectral line shape. Another convenient way to extract the dynamical information from the line shape is to obtain the inverse line width of the central resonance, $\langle \Delta H_0 \rangle^{-1}$, and the inverse second moment of the spectrum, $\langle H^2 \rangle^{-1}$, both of which have proven to be convenient experimental measures of the nitroxide mobility, hereafter called Hubbell plot.²⁶⁻²⁸ Figure 2B shows a Hubbell plot of the two measures of mobility for the 27 representative R1 side chains at positions in BAX in either 0 or 6 M GdnHCl. In a Hubbell plot, data points in the lower-left and upper-right corners indicate two extreme conditions, specifically, the mobility of the R1 side chain being extremely low and high, respectively. This study would like to emphasize that (Figure 2B) upon the addition of GdnHCl the distribution of red dots stands out with greater clarity in separation between the two populations (denoted by

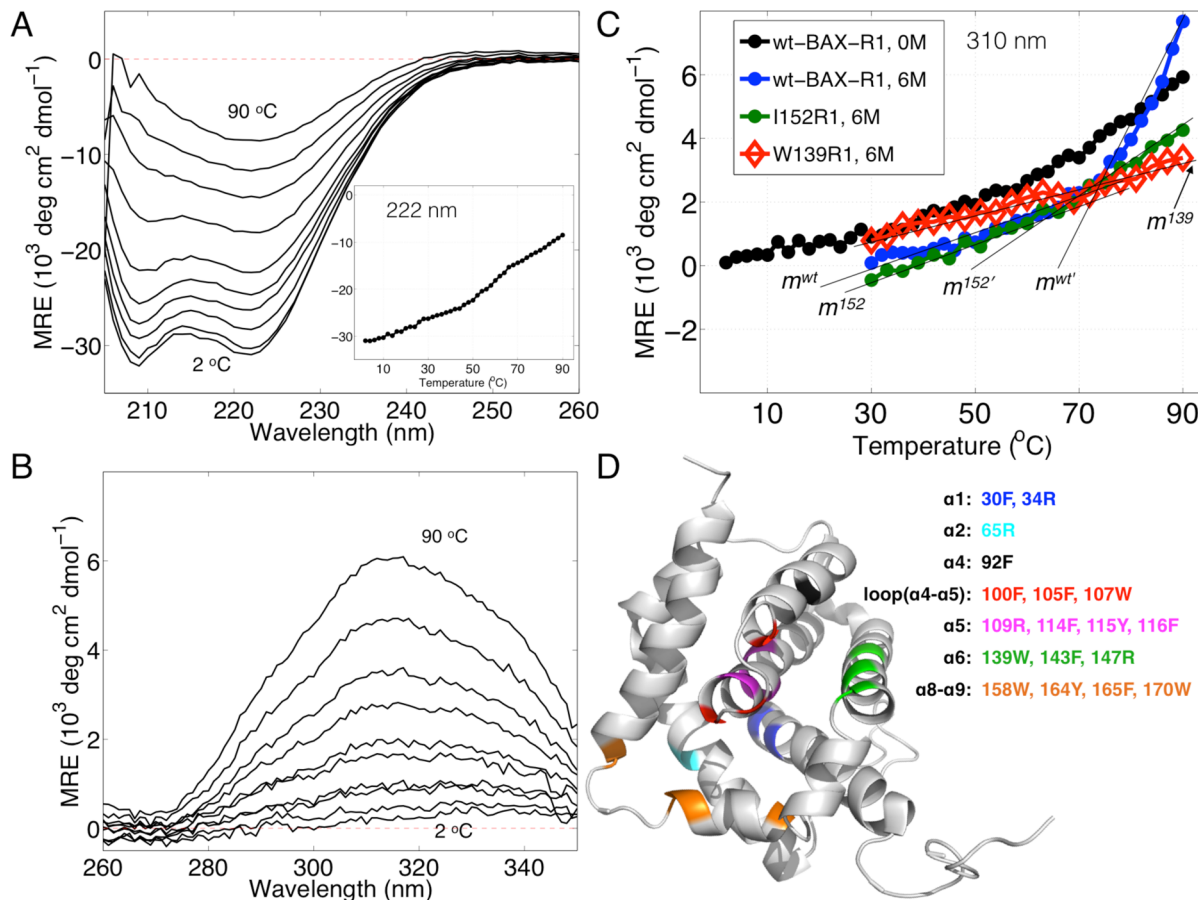


Figure 3. (A) Results of the thermal denaturation study of wt-BAX in the far-UV region by CD spectroscopy. It shows that BAX is not completely unfolded at high temperatures. The inset shows the mean residual ellipticity (MRE) at 222 nm concerning temperature (2–90 °C, in increments of 2 °C). There seems to be a melting transition around 70 °C in the results, albeit rather vague. (B) Results of the thermal denaturation study of wt-BAX in the near-UV region. The magnitude of the near-UV signal increases with increasing temperature, indicating the presence of significant aromatic interactions at high temperatures. (C) Variations of MRE at 310 nm of various BAX variants concerning temperature. The corresponding slopes of the solid thin lines (i.e., fits to the data) are 0.052(m^{wt}), 0.310($m^{wt'}$), 0.058(m^{152}), 0.107($m^{152'}$), and 0.038(m^{139}). (D) A cartoon model of BAX structure (PDB: 1f16) highlighting the residues that are identified to be involved in aromatic interactions within BAX. These residues are shown in colors according to different segments as noted.

dashed circles), showing that only at buried and some contact sites in the CTR do the residues cluster and remain in the left-hand-side circle, a region representing a highly immobilized state of the R1 side chain due to the dense packing in the interior of the protein. Among the drastic changes are the results of 94R1, 117R1, 142R1, and 164R1, which were observed to move into the left-hand-side circle, and the results of 25R1, 62R1, 63R1, and 76R1, which all belong to the NTR and were observed to move largely into the right-hand-side circle due to the unfolding of the NTR. The information revealed from the Hubbell plot (Figure 2B) is generally in accord with the result of hyperfine analysis that in high GdnHCl the NTR becomes denatured, but the CTR retains its local and tertiary structure. Moreover, in the CTR, there are four sites (99R1, 137R1, 152R1, and 161R1) whose spectra exhibit a (relatively) distinct increase in mobility and their corresponding values move from the left- to right-hand-side circles upon the presence of 6 M GdnHCl. The four sites are at the interface between the NTR and the CTR, and will be described further in the Discussion. Collectively, the ESR study demonstrates that the N- and C-terminal regions respond differently (in terms of local mobility of the side

chains, derived from the results in Figure 2) to the presence of GdnHCl.

Thermal Denaturation Study by CD Spectroscopy.

We have studied wt-BAX in the absence of GdnHCl at varying temperatures (from 2 to 90 °C in increments of 2 °C) by CD spectroscopy (Figure 3). All of the CD spectra presented are the results after subtraction of averaged blank spectra. The CD spectrum in the far-UV region at 2 °C (Figure 3A) exhibits a typical characteristic shape and minimum bands at 208 and 222 nm, indicative of the presence of α -helical structures as expected for wt-BAX. The magnitude of the CD signal at 208 and 222 nm is reduced with increasing temperature, indicating a decrease in the α -helical content of BAX. Interestingly, the CD spectrum corresponding to 90 °C is in no way similar to a spectrum of random coil, indicating that wt-BAX retains some secondary structure and does not completely unfold to a random coil at high temperatures, which is consistent with the previous study.¹⁷ The magnitude of CD signal at 222 nm is plotted against temperature and shown as an inset of Figure 3A, exhibiting a plausible melting temperature (T_m) around 70 °C, albeit rather vague and, therefore, not useful for further derivations of a folding constant from the result. However, the

CD spectra in the near-UV region (Figure 3B) reveal more molecular details of BAX. We observe a distinct increase in the magnitude of the near-UV signals with increasing temperature from 2 to 90 °C. The presence of significant near-UV signals is a good indication that the local chiral environment of aromatic side chains is enhanced, suggesting the predominance of tertiary interactions.^{14,29} Of note, the observed enhancement of near-UV signal with temperature remains significant even in the presence of the reducing agents (DTT and TCEP), verifying that the strong near-UV signal was not due to the formation of disulfide bonds. Collectively, the results of CD spectroscopy indicate that, as temperature increases from 2 to 90 °C in 0 M GdnHCl, the α -helical content of BAX is not reduced appreciably, and its secondary structure is retained somewhat while its tertiary contacts are gradually enhanced.

To further explore the origin of the strong signals in the near-UV region, we have recorded CD spectra for wt-BAX-R1, I152R1, and W139R1 (Figure 3C and Figure S8, Supporting Information) in 6 M GdnHCl. (Note that, because GdnHCl yields substantial noises in the far-UV region, we, therefore, only show the recorded CD spectra in the near-UV region.) Figure 3C shows a collection of the magnitude plots of the CD signals at 310 nm. Near-UV CD spectra are known to be useful “fingerprints” for comparisons of tertiary structures between mutated variants of a protein and have been invaluable in studies of intermediate states of proteins.^{29,30} The magnitudes of the CD signals at 310 nm for the four studied samples (Figure 3C) are very much increased with increasing temperature in either 0 or 6 M GdnHCl. Perhaps the most explicit indication of the results is that there exists an intermediate compact state of BAX and the compact of its tertiary structure is increased during heating. From a comparison of the CD spectra of wt-BAX between 0 and 6 M GdnHCl, the magnitude of the CD signals is distinctly reduced upon the presence of GdnHCl, likely because the NTR is unfolded in 6 M GdnHCl and, therefore, its chirality is lost somewhat, leading to the reduction in magnitude of the near-UV signals. Moreover, it shows that (i) there is a transition around 70 °C in the result of 6 M GdnHCl, which is characterized by two distinct slopes, 0.052 and 0.310 (denoted by m^{wt} and $m^{\text{wt}'}$, respectively), (ii) the slopes of the 0 and 6 M GdnHCl studies are similar to each other below 70 °C, and (iii) upon the unfolding of the NTR in 6 M GdnHCl, the local chiral environment of aromatic side chains in the CTR seems to be enhanced at high temperatures. The enhancement is much increased above 70 °C in 6 M GdnHCl, resulting in an increase of slope changing from m^{wt} to $m^{\text{wt}'}$. From the study of I152R1, its corresponding slope below 70 °C ($m^{152} \sim 0.058$) is close to m^{wt} and its slope is increased ($m^{152'} \sim 0.107$) above 70 °C. The reason for why the slope $m^{152'}$ is much less than $m^{\text{wt}'}$ is given in later sections. Upon substitution of one tryptophan with the R1 side chain (i.e., W139R1), the slope is further reduced ($m^{139} \sim 0.038$), verifying that the magnitude of CD signals around 310 nm is correlated with aromatic amino acids. A number of factors can influence the CD spectra of aromatic amino acids in the near-UV region. Among these are the rigidity of protein, with the more highly mobile side chains having lower intensities, and the nature of the environment in terms of hydrogen bonding, polar groups, chirality, and polarizability.^{14,30,31} Besides, the near-UV CD spectrum can be altered by interactions between aromatic amino acids which are especially significant if the

distance between them is less than 1 nm. We, therefore, attribute the presence of the strong near-UV signals to the tertiary contacts stabilized by aromatic interactions between side chains in the highly packed local environment of the CTR.

Estimation of Aromatic Interactions. BAX contains many aromatic residues. There are 6 Trp, 2 Tyr, and 9 Phe in the CTR of BAX, while there are only 2 Phe residues (but no Trp and Tyr) in the NTR. To examine the possible contributions of aromatic interactions to the structure, we have performed some calculations to predict the possible aromatic interactions (here, specifically for aromatic–aromatic and cation–pi interactions in the calculations) using the protein interaction calculator (PIC) and the CaPTURE program.^{9,32} A total of 12 aromatic pairs was identified in 18 residues within BAX, wherein two pairs (143F–147R and 65R–170W) were identified to be energetically significant (−2.43 and −3.45 kcal/mol, respectively) in cation–pi interactions. The residues identified to contribute the aromatic interactions within BAX are shown in colors with different helices and listed in Figure 3D. The 12 pairs are 30F–115Y, 30F–34R, 92F–116F, 92F–139W, 100F–143F, 100F–109R, 143F–147R, 105F–107W, 105F–109R, 114F–158W, 164Y–165F, and 65R–170W. (Note that, although the above calculations are based on the human BAX available on PDB as 1f16, all of the 18 residues are conserved between the mouse and human BAX. The two species only differ in 15 out of 192 residues (>92% identical), and most of the differences are in the NTR.) Among the 12 aromatic pairs, only one pair belongs to the NTR.

Determination of Melting Temperatures by ThermoFluor Assay. Because CD spectroscopy was not useful in determining T_m of the BAX variants even in the absence of GdnHCl (cf. Figure 3A), ThermoFluor assay was carried out to probe the thermal and chemical stability of BAX.^{13,15} Figure 4A shows the plots of the fluorescence intensity of ThermoFluor assay for wt-BAX at varying concentrations of GdnHCl. The T_m value is unambiguously determined from the derivative of the results to be 71.11 ± 0.35 , 59.29 ± 0.37 , 52.38 ± 0.23 , and 42.59 ± 0.15 °C for 0, 1, 2, and 3 M GdnHCl, respectively. As the GdnHCl concentration is ≥ 4 M, BAX is already in a partially unfolded state being readily bound with the fluorescence dye (Sypro Orange) at low temperatures, which, in turn, would make a large contribution to the baseline of the signal. As a result, it is not possible to unambiguously determine T_m at high concentrations of GdnHCl.

A plot of the T_m differences between the cysteine variants of BAX and the cf-BAX (in the absence of GdnHCl) is shown with the sequence number of the mutation sites in Figure 4B. (The experimental data are shown in Figure S9, Supporting Information.) Note that the T_m value for cf-BAX is 67.92 ± 0.18 °C, which is approximately 3 °C reduced from T_m of wt-BAX. Nine out of the 28 BAX variants were found to have a T_m reduction more than 5 °C from the T_m of cf-BAX. Particularly, four BAX variants corresponding to the mutation sites at 27, 113, 114, and 152 were found to have T_m reductions more than 10 °C. Figure 4C shows the spatial locations of the four residues (highlighted in red) that caused the large T_m reductions and also the locations of the residues (in blue) that were identified to be involved in the aromatic interactions as described in Figure 3D. It clearly shows that the four residues are buried within BAX, with their side chains

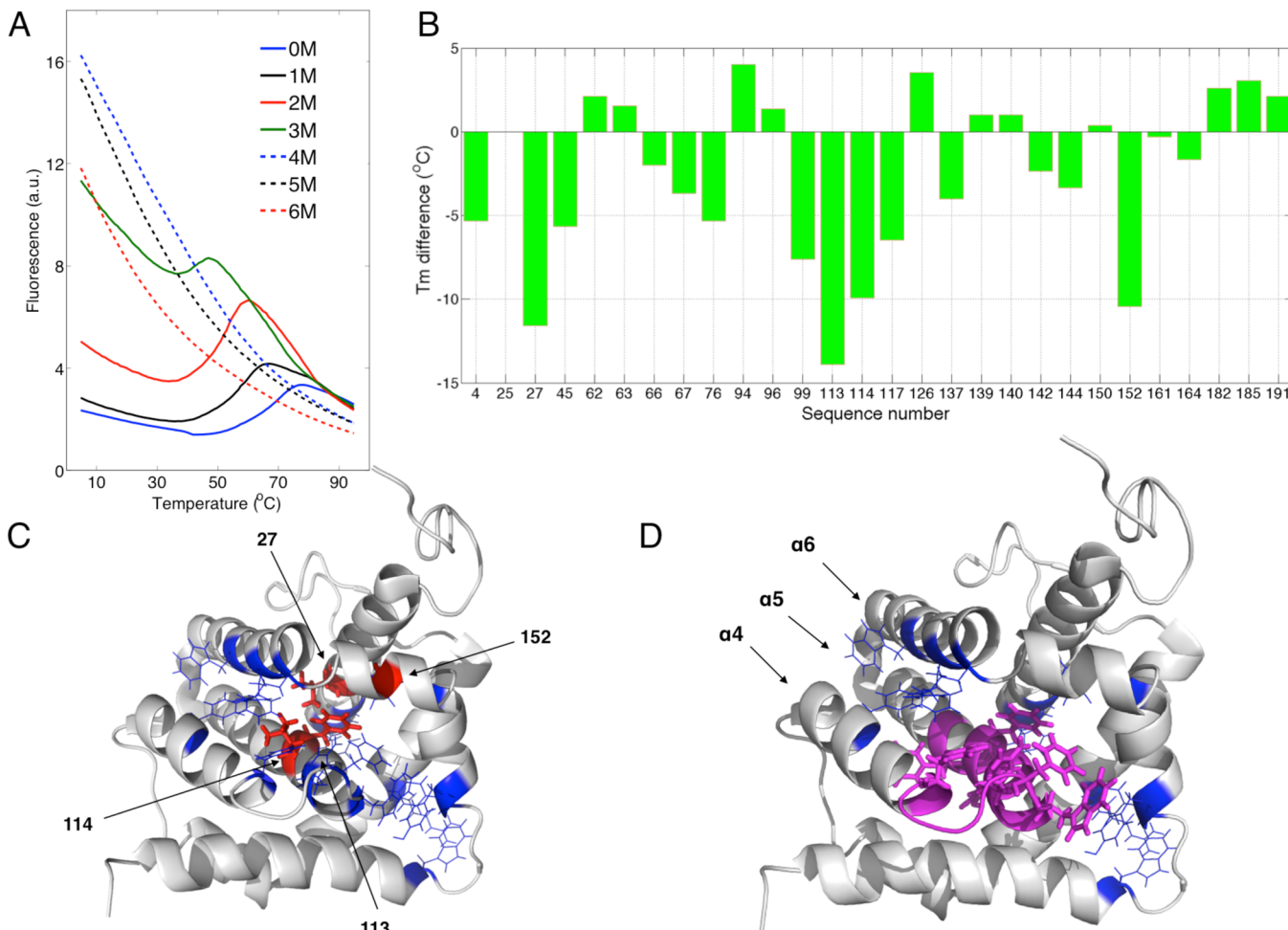


Figure 4. (A) Temperature-dependent fluorescence intensity of the ThermoFluor measurements for wt-BAX at 25 °C concerning GdnHCl concentration (0–6 M). The Tm value can only be unambiguously obtained for 0, 1, 2, and 3 M GdnHCl by the first derivative of the plots. (B) Tm difference between the indicated BAX variant and the cf-BAX, studied at 25 °C. A negative value indicates a Tm reduction, caused by the mutation site, from the Tm (67.92 ± 0.18 °C) of cf-BAX. (C) A model structure of BAX showing the residues (blue), which are identified to be involved in aromatic interactions, and the four residues (red), which (from the result in part B) cause large Tm reductions (>10 °C) after mutated to cysteine for spin labeling. The residues in red are pointing toward the same interior wherein aromatic interactions are highly involved within BAX. (D) The sequence from 99 to 117 is highlighted in magenta emphasizing that this segment plays a vital role in structural stabilization of BAX protein.

pointing toward an interior region wherein aromatic interactions are identified to be important. This finding provides a reasonable explanation for the large reduction of Tm in the study of the four BAX variants. It also explains why (Figure 3C) the slope of the near-UV signals of 152R1 was not largely increased (compared to the change from m^{wt} to $m^{\text{wt'}}$) as the temperature is above 70 °C. A point mutation at 152 disturbs the packing of CTR, making the CTR respond differently to GdnHCl. Another noteworthy feature in Figure 4B is that the cysteine variants from 99 to 117 seem to be an important region that a point mutation within the region could disrupt the stability of BAX substantially. Figure 4D shows a highlight of the region (residues 99–117 shown in magenta) wherein there are seven residues (i.e., 100, 105, 107, 109, 114, 115, and 116, whose side chains are highlighted in magenta) that were identified to be involved in the aromatic interactions in the analysis of Figure 3D. Taking the evidence of the ThermoFluor assays together, our results show that (i) the sequence numbering from 99 to 117 plays an important role in stabilizing BAX protein and (ii) the role of the aromatic interactions is evidently important in the stability of

BAX, as a large reduction in Tm can be induced with one point mutation within the core interior of BAX. Last, we note that the Tm determined in the ThermoFluor assay can only provide an assessment of the stability of tertiary structure as a whole, as the binding of the fluorescence dye to any of exposed hydrophobic surfaces on BAX would result in the observed fluorescence changes. The ThermoFluor results cannot provide specific information to discriminate the unfolding of the NTR and CTR.

GdnHCl-Induced Unfolding in the NTR and CTR. To probe the disruptions of the two structural regions, we prepared 62R1 and 139R1, which correspond to the NTR and CTR, respectively, in 3 M GdnHCl and carried out temperature-dependent cw-ESR measurements. The condition of 3 M GdnHCl is chosen because the ThermoFluor assays (Figure 4A) indicate that this condition is effective in lowering Tm to be less than 50 °C. Parts A and B of Figure 5 show ESR spectra of the 62R1 and 139R1, respectively, recorded at temperatures from 5 to 50 °C in increments of 5 °C. The spectra of 62R1 (Figure 5A) vary distinctly with temperature. Particularly, the low-field peak (indicated by a

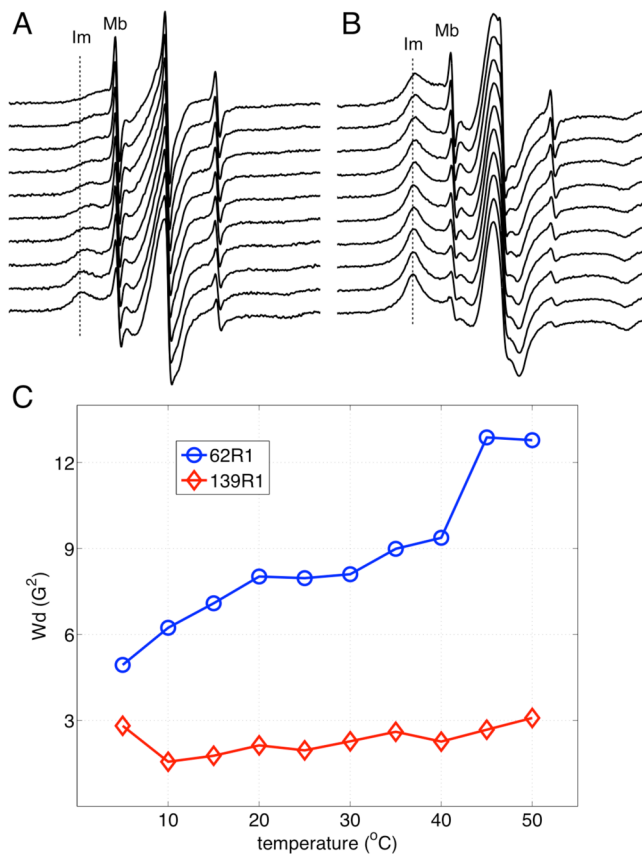


Figure 5. Cw-ESR spectra of 62R1 (A) and 139R1 (B), recorded in 3 M GdnHCl at varying temperatures from 5 °C (bottom) to 50 °C (top) in increments of 5 °C. The total scan width is 100 G. The (relatively) Mb and Im components are indicated. The population of the Mb decreases with increasing temperature in the 62R1 but not in the 139R1, indicating that the NTR is denatured and the CTR is resistant to thermal denaturation. (C) Temperature dependence of the normalized line width parameter W_d for the 62R1 and 139R1. Only the curve of the 62R1 displays a cooperativity-like transition with a midpoint in the range 40–45 °C, consistent with the ThermoFluor result.

broken line) in the spectra shows a clear shift toward higher field, suggesting that the mobility of the NTR is increased with increasing temperature. Nevertheless, relatively small changes with temperature were observed in the spectra of 139R1. Further analyses of the spectra were performed to yield a normalized line width parameter $W_d = (\Delta B_{\text{Mb}})^2 \times (h_{\text{Mb}}/h_{\text{Im}})$, where $(h_{\text{Mb}}/h_{\text{Im}})$ is the peak height ratio of the low-field resonances from the (relatively) mobile (Mb) and immobile (Im) spectral components and (ΔB_{Mb}) is the peak-to-peak line width of the low-field Mb, which is proportional to the ratio of integrated intensities of the two spectral components. This W_d parameter was previously demonstrated to be a useful indicator of local structural integrity during protein unfolding.³³ Figure 5C shows the temperature dependence of the W_d parameter. In 3 M GdnHCl, the W_d of the 139R1 varies relatively little with temperature, indicating that the population of the Mb spin-labels does not increase greatly as the temperature increases. On the other hand, the W_d of the 62R1 increases with increasing temperature, indicating that unfolding of the NTR leads to an increase in the population of the Mb at the expense of the Im component. A drastic change in the W_d of the 62R1 can

be clearly identified to occur between 40 and 45 °C, consistent with the T_m value determined in the ThermoFluor study. The results in Figure 5 provide further strong support for the NTR being denatured at high GdnHCl (or high temperatures) and the CTR being highly resistant to the denaturing effects.

DISCUSSION

This study has reported a comprehensive investigation on the stability of BAX against chemical and thermal denaturation using ESR, CD, and ThermoFluor spectroscopy methods. ESR spectra were collected from various sites covering all of the nine α -helices of BAX, providing information as to how the local environment along the nine helices is changed between 0 and 6 M GdnHCl. The site-specific ESR study shows that BAX can be divided into two distinct regions of structure, each of which responds differently to the chemical denaturation. In a solution containing 6 M GdnHCl, the NTR (i.e., the first 88 residues from the N-terminus) was found to unfold largely because the corresponding spectra became similar and exhibited a highly mobile state, whereas the CTR was found to retain to some extent its local structures and remain mostly packed. A majority of the spectra from the CTR even show an enhanced immobilization of the R1 side chain in 6 M GdnHCl (cf. Figure 2A), supporting a view that the CTR (covering from $\alpha 4$ to $\alpha 9$) retains a tertiary structure. This finding is evidently supported by the results of CD spectroscopy. The far-UV CD spectra confirm an appreciable amount of α -helical content of BAX in 0 M GdnHCl at high temperatures. Most importantly, the CD signal in the near-UV region was observed, in either 0 or 6 M GdnHCl, to be increased continuously with increasing temperature (Figure 3 and Figure S8, Supporting Information), suggesting the predominance of the tertiary interactions of the CTR within BAX. Our ThermoFluor assay shows that a point mutation in the interior surrounded by $\alpha 4$, $\alpha 5$, and $\alpha 6$ would disrupt (to some extent) the overall stability of BAX protein because the interior (particularly in the sequence from 99 to 117) is spatially crowded with residues involved in the aromatic–aromatic and cation–pi interactions. Reductions in T_m could be observed to be more than 5 °C for the point mutations in the core sequence from 99 to 117. As such, we conclude that an intermediate state of BAX protein (as illustrated in Figure 6A), which is composed of a coil-like denatured segment in the NTR and a structured core highly packed with the residues (highlighted in Figure 6A) involved in the aromatic interactions in the CTR, can likely exist as a stable monomer against the effects of the thermal and chemical denaturation. A comparison of the ESR spectra between 0 and 6 M GdnHCl (cf. Figure 1B) indicates that the vast majority of the local environments (buried or solvent-exposed) in the CTR are not drastically changed, suggesting that the cartoon structure in Figure 6A, which is directly taken from the reported NMR structure,¹⁶ can be a plausible model for the intermediate state. Further evidence to support this cartoon structure is shown in Figure 6B. As mentioned in Figure 2B, spectra from the four sites (99R1, 137R1, 152R1, and 161R1) in the CTR in 6 M GdnHCl exhibit a (relatively) distinct increase in mobility compared to 0 M GdnHCl. The four sites (highlighted in orange in Figure 6B) are at the interface between the NTR and the CTR. It, therefore, is reasonable to observe an increased mobility in these sites when the NTR is denatured in 6 M GdnHCl. The conformations of the CTR

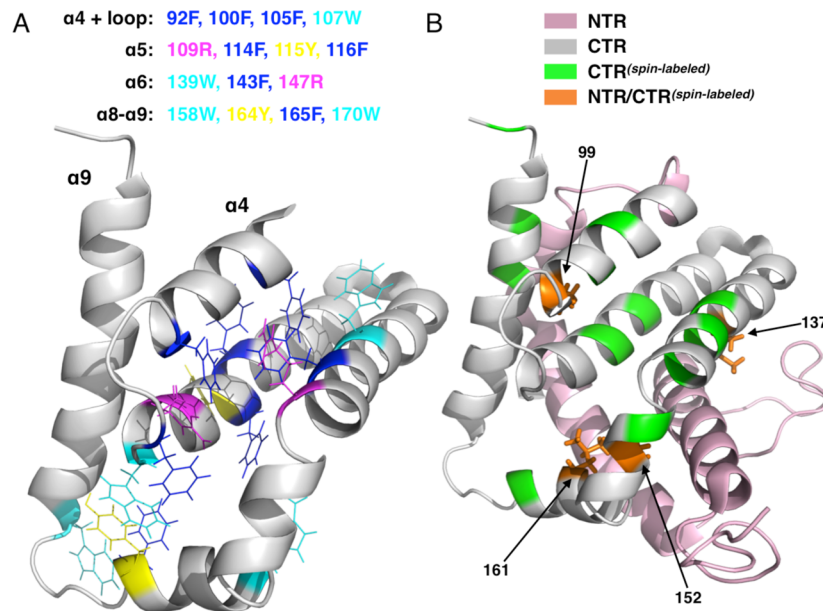


Figure 6. (A) A cartoon model illustrating a plausible intermediate state of BAX, in which the NTR is unfolded and, therefore, is not shown while the CTR (from $\alpha 4$ to $\alpha 9$) is likely structured and highly packed with the residues (F, W, Y, and R, as indicated by colors) that are involved in the aromatic interactions. It suggests that this highly stable intermediate state is stabilized by the aromatic interactions between side chains. (B) A cartoon model of BAX structure. All of the spin-labeled sites in the CTR (studied in Figure 1B) are shown in either green or orange. Those highlighted in orange are residues having side chains oriented on the interface between the CTR and the NTR. After the denaturation of the NTR, the four sites (orange) on the CTR are more exposed to solvent, resulting in a distinct increase in mobility as revealed in the Hubble plot (Figure 2B). This observation validates the cartoon model presented in part A.

between the native and intermediate states seem to be roughly similar, but further efforts to refine this cartoon structure are definitely needed. Moreover, we note that ESR spectra from the CTR could remain unchanged, being highly immobile and restricted, in 6 M GdnHCl for more than 2 weeks. This observation is taken as an important indication that the intermediate state is highly stable. Also, from the highly immobilized ESR line shapes that can be observed in many of the sites in the core region in 6 M GdnHCl, the side chains are highly packed without solvation of the core interior, suggesting that the stable state is likely a GdnHCl-induced compact-denatured state.^{34–37} This result implies the “direct interaction” mechanism for the effect of GdnHCl, since the formation of a partially folded intermediate is taken to be a major consequence of the direct-interaction model.³

This study has reported an observation of a highly stable intermediate state of BAX. The CTR is resistant to both the thermal and chemical denaturation, likely because its core interior is highly packed with aromatic and polar basic residues (cf. Figure 6A), which are identified to contribute the aromatic interactions in the area. The stabilizing effect appears to be important in maintaining the CTR and is increased with increasing temperature regardless of GdnHCl. Since the CTR is not unfolded upon the solvation of the hydrophobic interior by GdnHCl, the “indirect model” mechanism does not seem appropriate in this study of BAX unfolding. The high stability of the CTR is not simply due to the hydrophobicity of the residues.

CONCLUDING REMARKS

Normal denaturation is known to be driven principally by the gain of conformational entropy of side chains.^{1,38} This study shows that, upon thermal or chemical unfolding, the aromatic interactions to stabilize the side chains within the interior of

the CTR are rearranged, leading to an increase in the local chirality, thereby increasing the magnitude of near-UV signals. The mobility (or disordering) of the aromatic side chains is, therefore, decreased in the presence of the denaturing effects, leading to a decrease in the conformational entropy of the side chains within the core interior. This explains why the unfolding of the CTR is not favored in the thermal and chemical denaturation. Although hydrophobic interactions are generally considered the major determinant of protein stability, the results of this study draw attention to the important role of side-chain packing in protein stability. It is implied from the present study that the aromatic interactions (alternatively, side-chain packing in this study) can contribute at least as much to protein stability as more conventional interactions (e.g., hydrophobicity, hydrogen bonds, and salt bridges) and can be a major stabilizing force in determining protein stability and structures.

The present result may also provide an important implication for the biological function of the CTR of BAX. It was previously shown that the dissociation of $\alpha 5$ from $\alpha 6$ of BAX is a critical event in triggering the oligomerization of BAX that eventually leads to cell death.^{39,40} This dissociation is equivalent to the disruption of the core region of the CTR in the present study. As this dissociation is irreversible and fatal to a cell, a stringent regulation to initiate the BAX-mediated apoptosis is absolutely necessary. Our study has provided chemical insights into the origin of the exceptional stability of the CTR of BAX. These observations underscore the structural stability of BAX in serving its role as a gatekeeper for apoptosis.

■ ASSOCIATED CONTENT

§ Supporting Information

Figures S1–S9 showing cw-ESR spectra, theoretical fits, determination of hyperfine splitting in the spectra, size exclusion chromatography FPLC results, near-UV CD spectra, and plots of the temperature-dependent ThermoFluor measurements for all of the BAX mutants studied. This material is available free of charge via the Internet at <http://pubs.acs.org>.

■ AUTHOR INFORMATION

Corresponding Author

*E-mail: ywchiang@mx.nthu.edu.tw.

Notes

The authors declare no competing financial interest.

■ ACKNOWLEDGMENTS

This work was supported by Ministry of Science and Technology of Taiwan (102-2628-M-007-003-MY3 and 103-2627-M-007-005). All of the CW/pulse ESR measurements were conducted in the Research Instrument Center of Taiwan located at NTHU.

■ REFERENCES

- (1) Dill, K. A.; Alonso, D. O.; Hutchinson, K. Thermal Stabilities of Globular Proteins. *Biochemistry* **1989**, *28*, 5439–5449.
- (2) Vanzi, F.; Madan, B.; Sharp, K. Effect of the Protein Denaturants Urea and Guanidinium on Water Structure: A Structural and Thermodynamic Study. *J. Am. Chem. Soc.* **1998**, *120*, 10748–10753.
- (3) Hua, L.; Zhou, R.; Thirumalai, D.; Berne, B. J. Urea Denaturation by Stronger Dispersion Interactions with Proteins than Water Implies a 2-Stage Unfolding. *Proc. Natl. Acad. Sci. U. S. A.* **2008**, *105*, 16928–16933.
- (4) Myers, J. K.; Pace, C. N.; Scholtz, J. M. Denaturant M-Values and Heat-Capacity Changes: Relation to Changes in Accessible Surface Areas of Protein Unfolding. *Protein Sci.* **1995**, *4*, 2138–2148.
- (5) Wallqvist, A.; Covell, D. G.; Thirumalai, D. Hydrophobic Interactions in Aqueous Urea Solutions with Implications for the Mechanism of Protein Denaturation. *J. Am. Chem. Soc.* **1998**, *120*, 427–428.
- (6) Bennion, B. J.; Daggett, V. The Molecular Basis for the Chemical Denaturation of Proteins by Urea. *Proc. Natl. Acad. Sci. U. S. A.* **2003**, *100*, 5142–5147.
- (7) Pace, C. N. Determination and Analysis of Urea and Guanidine Hydrochloride Denaturation Curves. *Methods Enzymol.* **1986**, *131*, 266–280.
- (8) Bolen, D. W.; Rose, G. D. Structure and Energetics of the Hydrogen-Bonded Backbone in Protein Folding. *Annu. Rev. Biochem.* **2008**, *77*, 339–362.
- (9) Gallivan, J. P.; Dougherty, D. A. Cation-Π Interactions in Structural Biology. *Proc. Natl. Acad. Sci. U. S. A.* **1999**, *96*, 9459–9464.
- (10) Prajapati, R. S.; Sirajuddin, M.; Durani, V.; Sreeramulu, S.; Varadarajan, R. Contribution of Cation-Π Interactions to Protein Stability. *Biochemistry* **2006**, *45*, 15000–15010.
- (11) Dougherty, D. A. The Cation-Π Interaction. *Acc. Chem. Res.* **2013**, *46*, 885–893.
- (12) Fanucci, G. E.; Cafiso, D. S. Recent Advances and Applications of Site-Directed Spin Labeling. *Curr. Opin. Struct. Biol.* **2006**, *16*, 644–653.
- (13) Matulis, D.; Kranz, J. K.; Salemme, F. R.; Todd, M. J. Thermodynamic Stability of Carbonic Anhydrase: Measurements of Binding Affinity and Stoichiometry Using ThermoFluor. *Biochemistry* **2005**, *44*, 5258–5266.
- (14) Kelly, S. M.; Jess, T. J.; Price, N. C. How to Study Proteins by Circular Dichroism. *Biochim. Biophys. Acta, Proteins Proteomics* **2005**, *1751*, 119–139.
- (15) Vedadi, M.; Niesen, F. H.; Allali-Hassani, A.; Fedorov, O. Y.; Finerty, P. J.; Wasney, G. A.; Yeung, R.; Arrowsmith, C.; Ball, L. J.; Berglund, H.; et al. Chemical Screening Methods to Identify Ligands That Promote Protein Stability, Protein Crystallization, and Structure Determination. *Proc. Natl. Acad. Sci. U. S. A.* **2006**, *103*, 15835–15840.
- (16) Suzuki, M.; Youle, R. J.; Tjandra, N. Structure of Bax: Coregulation of Dimer Formation and Intracellular Localization. *Cell* **2000**, *103*, 645–654.
- (17) Yethon, J. A.; Epand, R. F.; Leber, B.; Epand, R. M.; Andrews, D. W. Interaction with a Membrane Surface Triggers a Reversible Conformational Change in Bax Normally Associated with Induction of Apoptosis. *J. Biol. Chem.* **2003**, *278*, 48935–48941.
- (18) Kuo, Y. H.; Tseng, Y. R.; Chiang, Y. W. Concurrent Observation of Bulk and Protein Hydration Water by Spin-Label ESR under Nanoconfinement. *Langmuir* **2013**, *29*, 13865–13872.
- (19) Fersht, A. R.; Petrovich, M. Reply to Campos and Munoz: Why Phosphate Is a Bad Buffer for Guanidinium Chloride Titrations. *Proc. Natl. Acad. Sci. U. S. A.* **2013**, *110*, E1244–E1245.
- (20) Budil, D. E.; Lee, S.; Saxena, S.; Freed, J. H. Nonlinear-Least-Squares Analysis of Slow-Motion EPR Spectra in One and Two Dimensions Using a Modified Levenberg-Marquardt Algorithm. *J. Magn. Reson., Ser. A* **1996**, *120*, 155–189.
- (21) Chiang, Y. W.; Otoshima, Y.; Watanabe, Y.; Inanami, O.; Shimoyama, Y. Dynamics and Local Ordering of Spin-Labeled Prion Protein: An ESR Simulation Study of a Highly PH-Sensitive Site. *J. Biomol. Struct. Dyn.* **2008**, *26*, 355–365.
- (22) Dzikowski, B.; Tipikin, D.; Freed, J. Conformational Distributions and Hydrogen Bonding in Gel and Frozen Lipid Bilayers: A High Frequency Spin-Label ESR Study. *J. Phys. Chem. B* **2012**, *116*, 6694–6706.
- (23) *Encyclopedia of Analytical Chemistry*; Meyers, R. A., Ed.; John Wiley & Sons, Ltd: Chichester, U.K., 2006.
- (24) Bordignon, E. Site-Directed Spin Labeling of Membrane Proteins. *Top. Curr. Chem.* **2012**, *321*, 121–157.
- (25) Drescher, M. EPR in Protein Science: Intrinsically Disordered Proteins. *Top. Curr. Chem.* **2012**, *321*, 91–119.
- (26) Hubbell, W. L.; Mchaourab, H. S.; Altenbach, C.; Lietzow, M. A. Watching Proteins Move Using Site-Directed Spin Labeling. *Structure* **1996**, *4*, 779–783.
- (27) Shabestari, M. H.; Wolfs, C. J. A. M.; Spruijt, R. B.; Van Amerongen, H.; Huber, M. Exploring the Structure of the 100 Amino-Acid Residue Long N-Terminus of the Plant Antenna Protein CP29. *Biophys. J.* **2014**, *106*, 1349–1358.
- (28) Mchaourab, H. S.; Lietzow, M. A.; Hideg, K.; Hubbell, W. L. Motion of Spin-Labeled Side Chains in T4 Lysozyme, Correlation with Protein Structure and Dynamics. *Biochemistry* **1996**, *35*, 7692–7704.
- (29) Clark, P. L.; Liu, Z. P.; Zhang, J.; Giersch, L. M. Intrinsic Tryptophans of CRABPI as Probes of Structure and Folding. *Protein Sci.* **1996**, *5*, 1108–1117.
- (30) Pain, R. Determining the CD Spectrum of a Protein. *Curr. Protoc. Protein Sci.* **2005**, *38*, 7.6.1–7.6.24.
- (31) Strickland, E. H. Aromatic Contributions to Circular Dichroism Spectra of Proteins. *CRC Crit. Rev. Biochem.* **1974**, *2*, 113–175.
- (32) Tina, K. G.; Bhadra, R.; Srinivasan, N. PIC: Protein Interactions Calculator. *Nucleic Acids Res.* **2007**, *35*, W473–W476.
- (33) Babavali, M.; Esmann, M.; Fedosova, N. U.; Marsh, D. Urea-Induced Unfolding of Na,K-ATPase as Evaluated by Electron Paramagnetic Resonance Spectroscopy. *Biochemistry* **2009**, *48*, 9022–9030.
- (34) Christensen, H.; Pain, R. H. Molten Globule Intermediates and Protein Folding. *Eur. Biophys. J.* **1991**, *19*, 221–229.

- (35) Jha, S. K.; Marqusee, S. Kinetic Evidence for a Two-Stage Mechanism of Protein Denaturation by Guanidinium Chloride. *Proc. Natl. Acad. Sci. U. S. A.* **2014**, *111*, 4856–4861.
- (36) Dolgikh, D. A.; Gilmanshin, R. I.; Brazhnikov, E. V.; Bychkova, V. E.; Semisotnov, G. V.; Venyaminov, S. Y.; Ptitsyn, O. B. A-Lactalbumin: Compact State with Fluctuating Tertiary Structure? *FEBS Lett.* **1981**, *136*, 311–315.
- (37) Freire, E. Thermodynamics of Partly Folded Intermediates in Proteins. *Annu. Rev. Biophys. Biomol. Struct.* **1995**, *24*, 141–165.
- (38) Dill, K. A.; Ozkan, S. B.; Shell, M. S.; Weikl, T. R. The Protein Folding Problem. *Annu. Rev. Biophys.* **2008**, *37*, 289–316.
- (39) Westphal, D.; Dewson, G.; Menard, M.; Frederick, P.; Iyer, S.; Bartolo, R.; Gibson, L.; Czabotar, P. E.; Smith, B. J.; Adams, J. M.; et al. Apoptotic Pore Formation Is Associated with in-Plane Insertion of Bak or Bax Central Helices into the Mitochondrial Outer Membrane. *Proc. Natl. Acad. Sci. U. S. A.* **2014**, *111*, E4076–E4085.
- (40) Czabotar, P. E.; Westphal, D.; Dewson, G.; Ma, S.; Hockings, C.; Fairlie, W. D.; Lee, E. F.; Yao, S. G.; Robin, A. Y.; Smith, B. J.; et al. Bax Crystal Structures Reveal How BH3 Domains Activate Bax and Nuclease Its Oligomerization to Induce Apoptosis. *Cell* **2013**, *152*, 519–531.